Title	Efficient computation of the impedance matrix of magnetic field integral equation for polyhedral conductors
Author(s)	Ni, Guyan; Shen, Zhongxiang; Shi, Jingfeng
Citation	Ni, G., Shen, Z., & Shi, J. (2015). Efficient computation of the impedance matrix of magnetic field integral equation for polyhedral conductors. IEEE transactions on antennas and propagation, 63(2), 630-635.
Date	2014
URL	http://hdl.handle.net/10220/25463
Rights	© 2014 IEEE. Personal use of this material is permitted. Permission from IEEE must be obtained for all other uses, in any current or future media, including reprinting/republishing this material for advertising or promotional purposes, creating new collective works, for resale or redistribution to servers or lists, or reuse of any copyrighted component of this work in other works. The published version is available at: [Article DOI: http://dx.doi.org/10.1109/TAP.2014.2384036].

Efficient Computation of the Impedance Matrix of Magnetic Field Integral Equation for Polyhedral Conductors

Guyan Ni, Zhongxiang Shen, Senior Member, IEEE, and Jingfeng Shi

***Abstract*—The vertical improper integral method is used to formulate a polyhedral magnetic field integral equation (MFIE), which can decrease the number of singular integrals compared with the traditional MFIE. Each element in the impedance matrix resulted from the equation's moment method solution based on Rao-Wilton-Glisson (RWG) basis function is divided into two parts: the induced surface current part and the scattered field part. We obtain the analytical expressions of the induced surface current part through mathematical manipulations, and indicate that some of the integrals in the scattered field part are zero and the remaining non-zero integrals are non-singular. These results can greatly improve the efficiency of the numerical solution. Numerical results show that our new method is more accurate and efficient than the traditional method in computing the impedance matrices.**

***Index Terms*—Magnetic field integral equation, method of moments, Rao-Wilton-Glisson basis function, scattered field, vertical improper integral.**

I. Introduction

BOTH electric field integral equation (EFIE) and magnetic field integral equation (MFIE) are widely used for electromagnetic scattering analysis of conducting objects with closed surfaces. In the solution of the MFIE or EFIE by the method of moments (MOM), the Rao-Wilton-Glisson (RWG) basis functions [6] are frequently used because of its accuracy and versatility. However, triangulating the surfaces of conducting bodies and using the RWG basis function to expand the unknown induced currents for the MFIE often give less accurate results compared with those of the EFIE [2], [8]. The key problem is the calculation of singular integrals associated with MFIE. In order to solve this problem, many techniques for treating singular integrals have been developed [4], such as the use of the solid-angle factor [2], singularity-extraction method [3], dual basis function method [7], evaluation the inner integral of the impedance matrix elements by its Taylor series [1]. However, if the conductor is a polyhedron, we find that many singular integrals in the MFIE solution are avoidable.

This work was supported by the National Natural Science Foundation of China (No.61171018) and Major State Basic Research Development Program of China (No.61319603).

G. Ni is with the College of Science, National University of Defense Technology, Changsha, Hunan 410073, China

Z. Shen is with School of Electrical and Electronic Engineering, Nanyang Technological University, Singapore, 639798

J. Shi is with Beijing Institute of Special Electromechanical Technology, Beijing 100012, China

In this paper, we introduce a novel and efficient technique to compute the MOM solution of the polyhedral MFIE with the use of RWG basis functions. We divide each impedance matrix element Z_{mn} of the MFIE into two parts: the induced surface current part Z_{mn}^J and the scattered field part Z_{mn}^s. We provide the closed-form expression of Z_{mn}^J by solving the planar triangular vector integral analytically, and deduce that some of integrals in Z_{mn}^s are zero and the remaining non-zero integrals are non-singular integrals by applying the vertical improper integral method [5]. Hence, the polyhedral MFIE can greatly decrease the number of singular integrals compared with the traditional MFIE method, and the analytical elements can also improve the efficiency of the numerical solution. Numerical results show that our new method is more accurate and efficient than the traditional method in computing the impedance matrices.

II. MFIE formulation

For a conducting scatterer with closed surface S, the traditional MFIE can be written from the boundary condition $\hat{n} \times (\mathbf{H}^i + \mathbf{H}^s) = \mathbf{J}_S$ as

$$\hat{n}(\mathbf{r}) \times \mathbf{H}^i(\mathbf{r}) = \frac{1}{2}\mathbf{J}_S(\mathbf{r}) - \hat{n}(\mathbf{r}) \times p.v. \iint_S \nabla g(\mathbf{r}, \mathbf{r}') \times \mathbf{J}_S(\mathbf{r}') dS', \quad (1)$$

where $\mathbf{r} \in S$, $p.v.$ denotes the Cauchy principal value integral, $g(\mathbf{r}, \mathbf{r}')$ is the Green's function defined as

$$g(\mathbf{r}, \mathbf{r}') = \frac{\exp(-jk|\mathbf{r} - \mathbf{r}'|)}{4\pi|\mathbf{r} - \mathbf{r}'|}, \ j = \sqrt{-1}. \quad (2)$$

However, if the conductor is a polyhedron and its surface S is formed by a number of small planar surfaces $\{T_n : n = 1, 2, \cdots, N\}$ with $\hat{n}_k$ being the unit normal pointing outward of T_k. Considering an observation point $\mathbf{r}_k \in T_k$, for $k = 1, 2, \cdots, N$ and based on the vertical improper integral [5], the tangential scattered magnetic field at $\mathbf{r}_k$ is as follows [5],

$$\hat{n}_k \times \mathbf{H}^s(\mathbf{r}_k) = \frac{\mathbf{J}_S(\mathbf{r}_k)}{2} + \sum_{n=1, n\neq k}^{N} \hat{n}_k \times \iint_{T_n} \left(\nabla g(\mathbf{r}, \mathbf{r}') \times \mathbf{J}_S(\mathbf{r}')\right) dS'. \quad (3)$$

Substituting (3) into the boundary condition, we obtain the

new MFIE based on the vertical improper integral.

$$\hat{n}_k \times \mathbf{H}^i(\mathbf{r}_k) = \frac{\mathbf{J}_S(\mathbf{r}_k)}{2} - \sum_{n=1,n\neq k}^{N} \hat{n}_k \times \iint_{T_n} (\nabla g(\mathbf{r},\mathbf{r}') \times \mathbf{J}_S(\mathbf{r}'))\, dS'. \quad (4)$$

Solutions of (1) and (4) with the MOM requires the expansion of $\mathbf{J}_S(\mathbf{r})$ into a series of basis functions and projection of the boundary condition onto testing functions. The RWG basis $\{\mathbf{f}_m(\mathbf{r})\}$ is defined in [6], as shown in Fig. 1.

$$\mathbf{f}_m(\mathbf{r}) = \begin{cases} \frac{(-1)^i l_m}{2A_{mi}}(\mathbf{r}-\mathbf{r}_{mi}), & \mathbf{r}\in S_{mi},\ i=1,2, \\ 0, & \text{otherwise}, \end{cases} \quad (5)$$

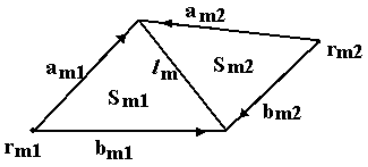

Fig. 1. The m-th triangle-pair of the RWG basis.

Use the RWG functions as the basis, and define $\mathbf{J}_S(\mathbf{r})$ as

$$\mathbf{J}_S(\mathbf{r}) = \sum_{n=1}^{M} a_n \mathbf{f}_n(\mathbf{r}), \quad (6)$$

where a_n is an unknown coefficient of the n-th basis functions.

At the same time, applying the RWG functions as test functions to (1) and (4), one can obtain the following $M \times M$ matrix equation

$$\sum_{n=1}^{M} (Z^J_{mn} - Z^s_{mn}) a_n = v_m, \quad m = 1, \cdots, M, \quad (7)$$

where

$$v_m = \iint_{S_{m1}\cup S_{m2}} (\hat{n}_m \times \mathbf{H}^i(\mathbf{r})) \cdot \mathbf{f}_m(\mathbf{r}) dS, \quad (8)$$

$$Z^J_{mn} = \frac{1}{2} \iint_{(S_{m1}\cup S_{m2})\cap(S_{n1}\cup S_{n2})} \mathbf{f}_n(\mathbf{r}) \cdot \mathbf{f}_m(\mathbf{r}) dS. \quad (9)$$

For the traditional MFIE,

$$Z^s_{mn} = \iint_S \left(\hat{n}(\mathbf{r}) \times p.v. \iint_S \nabla g(\mathbf{r},\mathbf{r}') \times \mathbf{f}_n(\mathbf{r}') dS' \right) \cdot \mathbf{f}_m(\mathbf{r}) dS. \quad (10)$$

In the new MFIE,we have

$$Z^s_{mn} = \sum_{k=1}^{N} \sum_{l=1,l\neq k}^{N} \iint_{T_k} (\hat{n}_k \times \iint_{T_l} \nabla g(\mathbf{r},\mathbf{r}') \times \mathbf{f}_n(\mathbf{r}') dS') \cdot \mathbf{f}_m(\mathbf{r}) dS. \quad (11)$$

In the following, we will derive analytical expressions of Z^J_{mn} and v_m. In addition, we will indicate that some integrals in Z^s_{mn} are zero and the remaining integrals are non-singular.

III. Analytical expressions

A. Three Basic Integrals

We first present the following three basic planar triangular vector integrals (12), (13) and (14), which are used in deriving the analytical expressions of Z^J_{mn} and v_m.

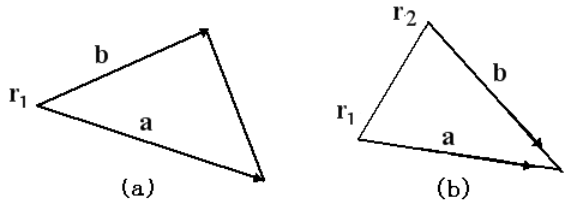

Fig. 2. Two kinds of planar triangles.

$$\iint_{S_\Delta} (\mathbf{r}-\mathbf{r}_1) dS = A(\mathbf{r}^c - \mathbf{r}_1) \quad (12)$$

$$\iint_{S_\Delta} (\mathbf{r}-\mathbf{r}_1)^2 dS = \frac{A}{6}[\mathbf{a}^2 + \mathbf{b}^2 + \mathbf{a}\cdot\mathbf{b}] \quad (13)$$

$$\iint_{S_\Delta} (\mathbf{r}-\mathbf{r}_1)\cdot(\mathbf{r}-\mathbf{r}_2) dS = \frac{A}{6}[3\mathbf{a}\cdot\mathbf{b} - \mathbf{a}^2 - \mathbf{b}^2] \quad (14)$$

where A denotes the area of S_Δ, $\mathbf{r}_1$ and $\mathbf{r}_2$ denote two different vertexes of S_Δ, $\mathbf{r}^c$ denotes the center point of S_Δ, (see Fig. 2(a) for (12) and (13), Fig. 2(b) for (14)).

Proof. (I) Assume that the triangle of Fig. 2(a) is uniformly partitioned into n triangles S_i, $(i = 1, 2, \cdots, n)$. Then for each triangle S_i, its area $\Delta S_i = A/n$. Let point $\mathbf{p}_i \in S_i$. We have

$$\begin{aligned} \iint_{S_\Delta} (\mathbf{r}-\mathbf{r}_1) dS &= \lim_{n\to\infty} \sum_{i=1}^{n} (\mathbf{p}_i - \mathbf{r}_1) \Delta S_i \\ &= \lim_{n\to\infty} \frac{A}{n} \sum_{i=1}^{n} (\mathbf{p}_i - \mathbf{r}_1) \\ &= A(\mathbf{r}^c - \mathbf{r}_1). \end{aligned} \quad (15)$$

(II) Assume that the triangle of Fig. 2(a) is partitioned like Fig. 3(a). For each parallelogram S_{ij} $(1 \le i \le n-1, 1 \le j \le n-i)$, choose a point $\mathbf{p}_{ij} \in S_{ij}$ as in Fig. 3(a). Then

$$\mathbf{p}_{ij} - \mathbf{r}_1 = \mathbf{a}(i-1)/n + \mathbf{b}(j-1)/n. \quad (16)$$

Each parallelogram S_{ij} has an area of $\Delta S_{ij} \approx \frac{2A}{n(n-1)}$. Hence,

$$\begin{aligned} \iint_{S_\Delta} (\mathbf{r}-\mathbf{r}_1)^2 dS &= \lim_{n\to\infty} \sum_{i=1}^{n-1} \sum_{j=1}^{n-i} (\mathbf{p}_{ij} - \mathbf{r}_1)^2 \Delta S_{ij} \\ &= \lim_{n\to\infty} \frac{2A}{n^3(n-1)} \sum_{i=1}^{n-1} \sum_{j=1}^{n-i} [(i-1)^2\mathbf{a}^2 \\ &\quad + (j-1)^2\mathbf{b}^2 + 2(i-1)(j-1)\mathbf{a}\cdot\mathbf{b}] \\ &= \frac{A}{6}(\mathbf{a}^2 + \mathbf{b}^2 + \mathbf{a}\cdot\mathbf{b}) \end{aligned} \quad (17)$$

(III) Assume that the triangle of Fig. 2(b) is also partitioned like Fig. 3(b). For each parallelogram S_{ij} $(1 \le i \le n-1, 1 \le$

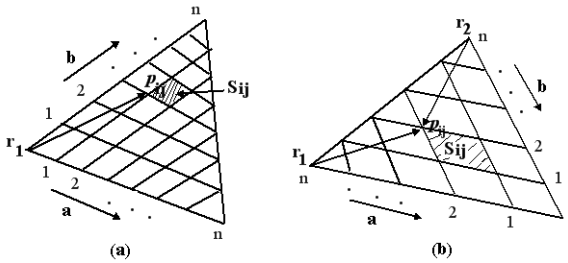

Fig. 3. Two partitioned triangles.

$j \le n-i$), choose a point $\mathbf{p}_{ij} \in S_{ij}$ as in Fig. 3(b). Then

$$\mathbf{p}_{ij} - \mathbf{r}_1 = \mathbf{a}(n-i)/n - \mathbf{b}j/n, \quad (18)$$
$$\mathbf{p}_{ij} - \mathbf{r}_2 = -\mathbf{a}i/n + \mathbf{b}(n-j)/n. \quad (19)$$

Each parallelogram S_{ij} area $\Delta S_{ij} \approx \frac{2A}{n(n-1)}$. Hence,

$$\begin{aligned}
&\iint_{S_\Delta} (\mathbf{r}-\mathbf{r}_1)\cdot(\mathbf{r}-\mathbf{r}_2)dS \\
&= \lim_{n\to\infty} \sum_{i=1}^{n-1}\sum_{j=1}^{n-i} (\mathbf{p}_{ij}-\mathbf{r}_1)\cdot(\mathbf{p}_{ij}-\mathbf{r}_2)\Delta S_{ij} \\
&= \lim_{n\to\infty} \frac{2A}{n^3(n-1)} \sum_{i=1}^{n-1}\sum_{j=1}^{n-i} (\mathbf{a}(n-i) \\
&\quad -\mathbf{b}j)\cdot(-\mathbf{a}i + \mathbf{b}(n-j)) \\
&= \frac{A}{6}[3\mathbf{a}\cdot\mathbf{b} - \mathbf{a}^2 - \mathbf{b}^2]. \quad (20)
\end{aligned}$$

This completes the proof. □

B. Computation of v_m

Using (8) and (12), we have

$$\begin{aligned}
v_m &\approx (\hat{n}_{m1}\times\mathbf{H}^i(\mathbf{r}^c))\cdot\iint_{S_{m1}} \mathbf{f}_m(\mathbf{r})dS \\
&\quad +(\hat{n}_{m2}\times\mathbf{H}^i(\mathbf{r}^c))\cdot\iint_{S_{m2}} \mathbf{f}_m(\mathbf{r})dS \\
&= (\hat{n}_{m1}\times\mathbf{H}^i(\mathbf{r}^c_{m1}))\cdot\mathbf{f}_m(\mathbf{r}^c_{m1})A_{m1} \\
&\quad +(\hat{n}_{m2}\times\mathbf{H}^i(\mathbf{r}^c_{m2}))\cdot\mathbf{f}_m(\mathbf{r}^c_{m2})A_{m2} \quad (21)
\end{aligned}$$

where $\mathbf{r}^c_{m1} and\ \mathbf{r}^c_{m2}$ denote the center points of S_{m1} and S_{m2} respectively, $A_{m1} and\ A_{m2}$ denote areas of S_{m1} and S_{m2}, respectively.

C. Computation of Z^J_{mn}

1) If $m = n$, using (9) and (13), we obtain

$$\begin{aligned}
Z^J_{mm} &= \frac{1}{2}\iint_{S_{m1}} \mathbf{f}_m(\mathbf{r})\cdot\mathbf{f}_m(\mathbf{r})\mathrm{d}S \\
&\quad +\frac{1}{2}\iint_{S_{m2}} \mathbf{f}_m(\mathbf{r})\cdot\mathbf{f}_m(\mathbf{r})\mathrm{d}S \\
&= \frac{1}{2}\iint_{S_{m1}} \left(\frac{l_m}{2A_{m1}}\right)^2(\mathbf{r}-\mathbf{r}_{m1})^2\mathrm{d}S \\
&\quad +\frac{1}{2}\iint_{S_{m2}} \left(\frac{l_m}{2A_{m2}}\right)^2(\mathbf{r}-\mathbf{r}_{m2})^2\mathrm{d}S \\
&= \frac{l_m^2}{48A_{m1}}[\mathbf{a}^2_{m1}+\mathbf{b}^2_{m1}+\mathbf{a}_{m1}\cdot\mathbf{b}_{m1}] \\
&\quad +\frac{l_m^2}{48A_{m2}}[\mathbf{a}^2_{m2}+\mathbf{b}^2_{m2}+\mathbf{a}_{m2}\cdot\mathbf{b}_{m2}] \quad (22)
\end{aligned}$$

where vectors $\mathbf{a}_{m1},\ \mathbf{b}_{m1},\ \mathbf{a}_{m2}$ and $\mathbf{b}_{m2}$ are defined in Fig. 1.

2) If $m \neq n$ and $(S_{m1}\cup S_{m2})\cap(S_{n1}\cup S_{n2}) = \phi$, then

$$Z^J_{mn} = 0. \quad (23)$$

3) If $m \neq n$ and $S_{mi} = S_{nj},\ i,j = 1$ or 2, then using (9) and (14), we obtain

$$\begin{aligned}
Z^J_{mn} &= \frac{1}{2}\iint_{S_{mi}} \mathbf{f}_n(\mathbf{r})\cdot\mathbf{f}_m(\mathbf{r})\mathrm{d}S \\
&= \frac{1}{2}\iint_{S_{mi}} \frac{(-1)^{j+1}l_n}{2A_{nj}}(\mathbf{r}-\mathbf{r}_{nj})\cdot\frac{(-1)^{i+1}l_m}{2A_{mi}}(\mathbf{r}-\mathbf{r}_{mi})\mathrm{d}S \\
&= \frac{(-1)^{i+j}l_nl_m}{8A_{nj}A_{mi}}\iint_{S_{mi}} (\mathbf{r}-\mathbf{r}_{nj})\cdot(\mathbf{r}-\mathbf{r}_{mi})\mathrm{d}S \\
&= \frac{(-1)^{i+j}l_nl_m}{48A_{mi}}[3\mathbf{a}_{mi}\cdot\mathbf{b}_{nj} - \mathbf{a}^2_{mi} - \mathbf{b}^2_{nj}] \quad (24)
\end{aligned}$$

where $\mathbf{a}_{mi} = \mathbf{r}_{mn} - \mathbf{r}_{mi}$, $\mathbf{b}_{nj} = \mathbf{r}_{mn} - \mathbf{r}_{nj}$, as shown in Fig. 4.

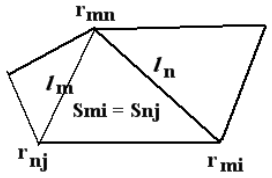

Fig. 4. Two triangle-pairs with $S_{mi} = S_{nj}$.

D. Computation of Z^s_{mn}.

Using (5), we rewrite Z^s_{mn} as

$$Z^s_{mn} = \sum_{i,j=1}^{2} Z^s_{mi\ nj}, \quad (25)$$

where $Z^s_{mi\ nj}$ is given in the following.

(I) The traditional MFIE case.

1) If $S_{mi} = S_{nj}$, then

$$\begin{aligned}
Z^s_{mi\ nj} &= \iint_{S_{mi}} (\hat{n}(\mathbf{r})\times p.v.\iint_{S_{nj}} \nabla g(\mathbf{r},\mathbf{r}') \\
&\quad \times\mathbf{f}_n(\mathbf{r}')dS')\cdot\mathbf{f}_m(\mathbf{r})dS. \quad (26)
\end{aligned}$$

This is a singular integral.

2) Else

$$Z^s_{mi\ nj} = \iint_{S_{mi}} (\hat{n}(\mathbf{r}) \times \iint_{S_{nj}} \nabla g(\mathbf{r},\mathbf{r}') \times \mathbf{f}_n(\mathbf{r}')dS') \cdot \mathbf{f}_m(\mathbf{r})dS. \quad (27)$$

This is a normal integral.

(II) The new MFIE case.

Let $\mathbf{r} \in S_{mi}$, $\mathbf{r}' \in S_{nj}$, and $\hat{n}_{mi}$ be the unit normal pointing outward of S_{mi}.

1) If S_{mi} and S_{nj} in the same planar surface T_k ($k = 1, \cdots, N$), then $\hat{n}_{mi} \times ((\mathbf{r}-\mathbf{r}') \times \mathbf{J}_S(\mathbf{r}')) = \mathbf{0}$. It follows that $\hat{n}_{mi} \times (\nabla g(\mathbf{r},\mathbf{r}') \times \mathbf{f}_n(\mathbf{r}')) = \mathbf{0}$. Hence,

$$Z^s_{mi\ nj} = 0. \quad (28)$$

2) Else

$$Z^s_{mi\ nj} = \iint_{S_{mi}} (\hat{n}_{mi} \times \iint_{S_{nj}} \nabla g(\mathbf{r},\mathbf{r}') \times \mathbf{f}_n(\mathbf{r}')\mathrm{d}S') \cdot \mathbf{f}_m(\mathbf{r})\mathrm{d}S. \quad (29)$$

This is again a normal integral.

IV. Numerical Examples

A. Comparison of Approximate and Analytic Solutions

In the numerical computation of MFIE, many researchers take the central points $\mathbf{r}^c$ of triangles to compute of integrals (12), (13) and (14) as their approximate values. Let

$$I_0 = \iint_{S_\Delta} (\mathbf{r}^c - \mathbf{r}_1)dS = A(\mathbf{r}^c - \mathbf{r}_1), \quad (30)$$

$$I_1 = \iint_{S_\Delta} (\mathbf{r}^c - \mathbf{r}_1)^2 dS = A(\mathbf{r}^c - \mathbf{r}_1)^2, \quad (31)$$

$$I_2 = \iint_{S_\Delta} (\mathbf{r}^c - \mathbf{r}_1) \cdot (\mathbf{r}^c - \mathbf{r}_2)dS = A(\mathbf{r}^c - \mathbf{r}_1) \cdot (\mathbf{r}^c - \mathbf{r}_2). \quad (32)$$

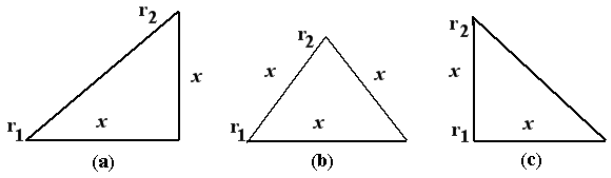

Fig. 5. Three kinds of integral triangles.

It is clear that I_0 is equal to the integral given in (12). But I_1 aNd I_2, are, in fact, incorrect. Next, we will compare approximate values I_1 and I_2 to analytic solutions (13) and (14) with three different shape triangles, as shown in Fig. 5.

We compute analytical solutions of (13) and I_1 for $x = 1,\ 0.1,\ 0.01$, respectively, as shown in Table 1. Similarly, we compute analytical solutions of (14) and I_2 for $x = 1,\ 0.1,\ 0.01$, respectively, and they are given in Table 2.

Tables 1 and 2 show that I_1 and I_2 cannot approximate (13) and (14), respectively, even if x is very small. The last columns of Tables 1 and 2 indicate that different shapes produce different errors. Hence, the solution of MFIE is more accurate if one uses the analytical solutions of Z^J_{mn} than I_1 and I_2.

Table 1. Integral (13) and I_1 for different shape triangles.

Δ	x	Int (13)	I_1	$\frac{\text{Int (13)}-I_1}{I_1}$
a	1	0.333	0.278	0.2
	0.1	3.33×10^{-5}	2.78×10^{-5}	0.2
	0.01	3.33×10^{-9}	2.79×10^{-9}	0.2
b	1	0.180	0.144	0.25
	0.1	1.80×10^{-5}	1.44×10^{-5}	0.25
	0.01	1.80×10^{-9}	1.44×10^{-9}	0.25
c	1	0.167	0.111	0.5
	0.1	1.67×10^{-5}	1.11×10^{-5}	0.5
	0.01	1.67×10^{-9}	1.11×10^{-9}	0.5

Table 2. Integral (14) and I_2 for different shape triangles.

Δ	x	Int (14)	I_2	$\frac{\text{Int}(14)-I_2}{I_2}$
a	1	0	-5.56×10^{-2}	-1
	0.1	0	-5.56×10^{-6}	-1
	0.01	0	-5.56×10^{-10}	-1
b	1	-3.60×10^{-2}	-7.22×10^{-2}	-0.5
	0.1	-3.60×10^{-6}	-7.22×10^{-6}	-0.5
	0.01	-3.60×10^{-10}	-7.22×10^{-10}	-0.5
c	1	-1.67×10^{-1}	-2.22×10^{-1}	-0.25
	0.1	-1.67×10^{-5}	-2.22×10^{-5}	-0.25
	0.01	-1.67×10^{-9}	-2.22×10^{-9}	-0.25

The next example we consider is the electromagnetic scattering by a perfectly electric conducting (PEC) cube and a PEC tetrahedron with a side length 0.1λ, where λ denotes the free-space wavelength. We calculate its bistatic radar cross-section (RCS) for both vertical and horizontal polarizations. Numerical results show that RCS results with the analytical solution are different from those obtained from I_1 and I_2, as shown in Fig. 6.

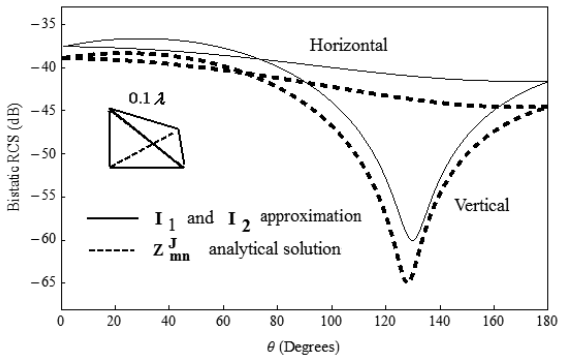

Fig. 6. Bistatic RCS of a PEC tetrahedron between analytical solution and approximate solution.

B. Comparison of Impedance Matrices

For the new MFIE, we have that $Z^s_{mi\ nj} = 0$ if S_{mi} and S_{nj} in the same planar surface, which implies that $Z^s_{mi\ nj} = 0$ if $S_{mi} = S_{nj}$. However, for the traditional MFIE, $Z^s_{mi\ nj}$ is a singular integral if $S_{mi} = S_{nj}$. In the following, we compare

the difference of two impedance matrices obtained by using two MFIEs, respectively.

For example, we consider the electromagnetic scattering by a PEC cube with a side length 0.2λ, where λ denotes the free-space wavelength. We partition the surface of the cube with 300 triangles and have 450 triangle-pairs. We compute the impedance matrices Z_1 based on the traditional MFIE, Z_2 based on the new MFIE, and their error matrix $Z_3 = Z_1 - Z_2$. Two matrices $\mathbf{A}$ and $\mathbf{B}$ are presented in the following. $\mathbf{A}$ is the submatrix of the first 6 columns and 6 rows of Z_1 and $\mathbf{B}$ is the submatrix of the first 6 columns and 6 rows of Z_3. It shows that elements of Z_1 and Z_2 are about from 10^{-4} to 10^{-7}, but elements of Z_3 are about from 10^{-13} to 10^{-16}. Indeed, the results from these two kinds of Z_{mn} are in good agreement, as shown in Fig. 7. Hence, the singular integrals of the traditional MFIE in the numerical computation based on the MOM can be avoided.

$$\mathrm{A} = \begin{pmatrix} 2.04\times10^{-4} & 2.34\times10^{-5} & 6.71\times10^{-5} & 2.23\times10^{-6} & 9.60\times10^{-8} & 4.07\times10^{-6} \\ 2.37\times10^{-5} & 2.34\times10^{-4} & 7.88\times10^{-5} & 1.18\times10^{-6} & 4.81\times10^{-6} & 1.14\times10^{-7} \\ 6.85\times10^{-5} & 7.80\times10^{-5} & 1.87\times10^{-4} & 1.86\times10^{-6} & 3.75\times10^{-7} & 2.39\times10^{-6} \\ 1.79\times10^{-6} & 1.92\times10^{-6} & 1.51\times10^{-6} & 2.11\times10^{-4} & 3.45\times10^{-5} & 5.68\times10^{-5} \\ 5.78\times10^{-9} & 4.36\times10^{-6} & 2.33\times10^{-7} & 3.45\times10^{-5} & 2.13\times10^{-4} & 5.47\times10^{-5} \\ 2.98\times10^{-6} & 1.03\times10^{-6} & 1.20\times10^{-6} & 5.67\times10^{-5} & 5.51\times10^{-5} & 1.69\times10^{-4} \end{pmatrix}$$

$$\mathrm{B} = \begin{pmatrix} 1.38\times10^{-16} & 0 & 0 & 1.94\times10^{-16} & 0 & 0 \\ 0 & 1.11\times10^{-16} & 0 & 0 & 0 & 0 \\ 0 & 0 & 4.44\times10^{-16} & 0 & 0 & 0 \\ 4.55\times10^{-13} & 0 & 0 & 2.22\times10^{-16} & 0 & 0 \\ 0 & 0 & 0 & 0 & 6.66\times10^{-16} & 0 \\ 0 & 0 & 0 & 0 & 0 & 6.66\times10^{-16} \end{pmatrix}$$

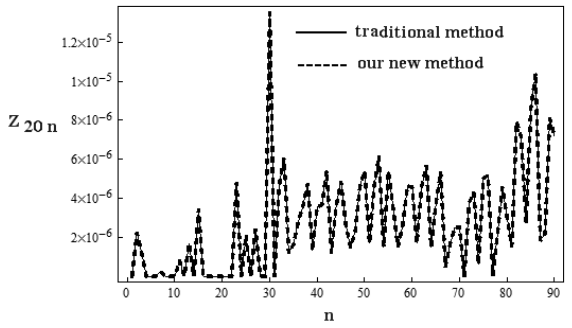

Fig. 7. Numerical results of Z^s_{mn} between the traditional method and our new method.

C. Comparison of CPU Time

For the same example as above, we partition the surface of the cube with 300 triangles and have 450 triangle-pairs. There are 810000 integrals to be computed in evaluating Z^s_{mn} by the traditional MFIE method, including 2700 singular integrals. However, there are only 675000 integrals, 83.3% of the total integrals, to be computed if we use the new MFIE method, and all these integrals are regular integrals. The CPU time used by two different methods in computing the impedance matrix is 5.58s by the traditional method and 1.29s by the new method, respectively.

In order to compare the computation time of two methods, we consider PEC cubes with their side length varying from 0.1λ to 1λ and the partition length is 0.05λ. Numerical result shows that the CPU time used by our new method is much shorter than by traditional method in computing impedance matrices, as shown in Fig. 8.

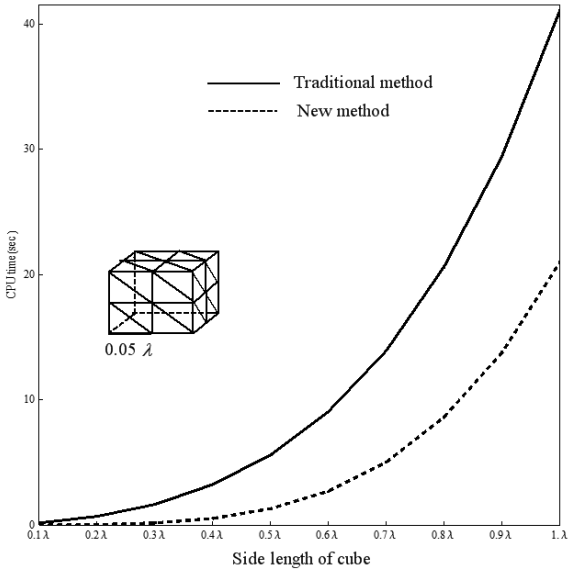

Fig. 8. CPU time required for PEC cubes between the traditional method and our new method.

V. Conclusion

In this paper, the vertical improper integral method has been introduced to compute the impedance matrices of polyhedral MFIE. Each impedance matrix element of the polyhedral MFIE is divided into two parts: the induced surface current part Z^J_{mn} and the scattered field part Z^s_{mn}. Three basic planar triangular vector integral formulations have been presented first and the analytical expressions of v_m and Z^J_{mn} have been derived. Numerical examples have shown that it is more accurate to compute the RCS by these analytical expressions than traditional methods. Second, we have rewritten Z^s_{mn} as $\sum_{i,j=1}^{2} Z^s_{mi\ nj}$, and indicated that $Z^s_{mi\ nj} = 0$ if S_{mi} and S_{nj} in the same planar surface T_k $(k = 1, \cdots, N)$, which implies that each integral of Z^s_{mn} is either zero or a regular integral. Comparing with the traditional MFIE, our new method can decrease the number of integrals, especially decrease the number of singular integrals, which in turn reduces the computational time. It may be mentioned that the results may also be used in other general MFIEs.

Acknowledgments

The authors would like to thank three anonymous reviewers for their valuable comments that greatly improved the manuscript.

References

[1] J. S. Asvestas, D. W. Richardson, and O. E. Allen, "Calculation of the impedance matrix inner integral of the magnetic-field integral equation to prescribed precision files," *IEEE Trans. Antennas Propag.*, vol. 61, pp. 5553-5558, Nov. 2013.

[2] Ö. Ergül, and L.Gürel, "Solid-angle factor in the magneticfield integral equation," *Microw. Opt. Technol. Lett.*, vol. 45, pp. 452-455, June 2005.
[3] L.Gürel and Ö. Ergül, "Singularity of the magnetic-field integral equation and its extraction," *IEEE Antennas and Wireless Propagation Letters*, vol.4, pp. 229-232, 2005
[4] J. Kataja, A. G. Polimeridis, J. R. Mosig, and Pasi Ylä-Oijala, "Analytical shape derivatives of the MFIE system matrix discretized with RWG functions," *IEEE Trans. Antennas Propag.*, vol. 60, pp. 985-988, February 2013.
[5] G. Ni, C. Yu, M. Bai and Y. He, "The convergence of the tangential scattered magnetic field based on the vertical improper integral," *Electromagnetics*, vol. 33, pp. 116-130, 2013.
[6] S. M. Rao, D. R. Wilton, and A. W. Glisson, "Electromagnetic scattering by surfaces of arbitrary shape," *IEEE Trans. Antennas Propag.*, vol. APC30, no. 3, pp. 409-418, May 1982.
[7] M. S. Tong and W. C. Chew, "New formulations for evaluating hypersingular and strongly singular integrals in electromagnetic integral equations," *IEEE AP-S International Symposium*, July 2010.
[8] L. Zhang A. Deng and M. Wang, "Improving the accuracy of the magnetic field integral equation with the use of a new impedance matrix element formulation," *IET Microw. Antennas Propag.*, vol. 3, pp. 850-855, August 2009